Science Advances
AAAS

Supplementary Materials for

ACSL6-activated IL-18R1–NF-κB promotes IL-18–mediated tumor immune evasion and tumor progression

Yuqin Di *et al.*

Corresponding author: Ziyang Wang, wangzy256@mail.sysu.edu.cn; Ligong Lu, luligong1969@jnu.edu.cn; Xiongjun Wang, xjwang02@sibcb.ac.cn; Weiling He, hewling@mail.sysu.edu.cn

Sci. Adv. **10**, eadp0719 (2024)
DOI: 10.1126/sciadv.adp0719

The PDF file includes:

Figs. S1 to S8
Tables S1 to S4
Legend for data S1

Other Supplementary Material for this manuscript includes the following:

Data S1

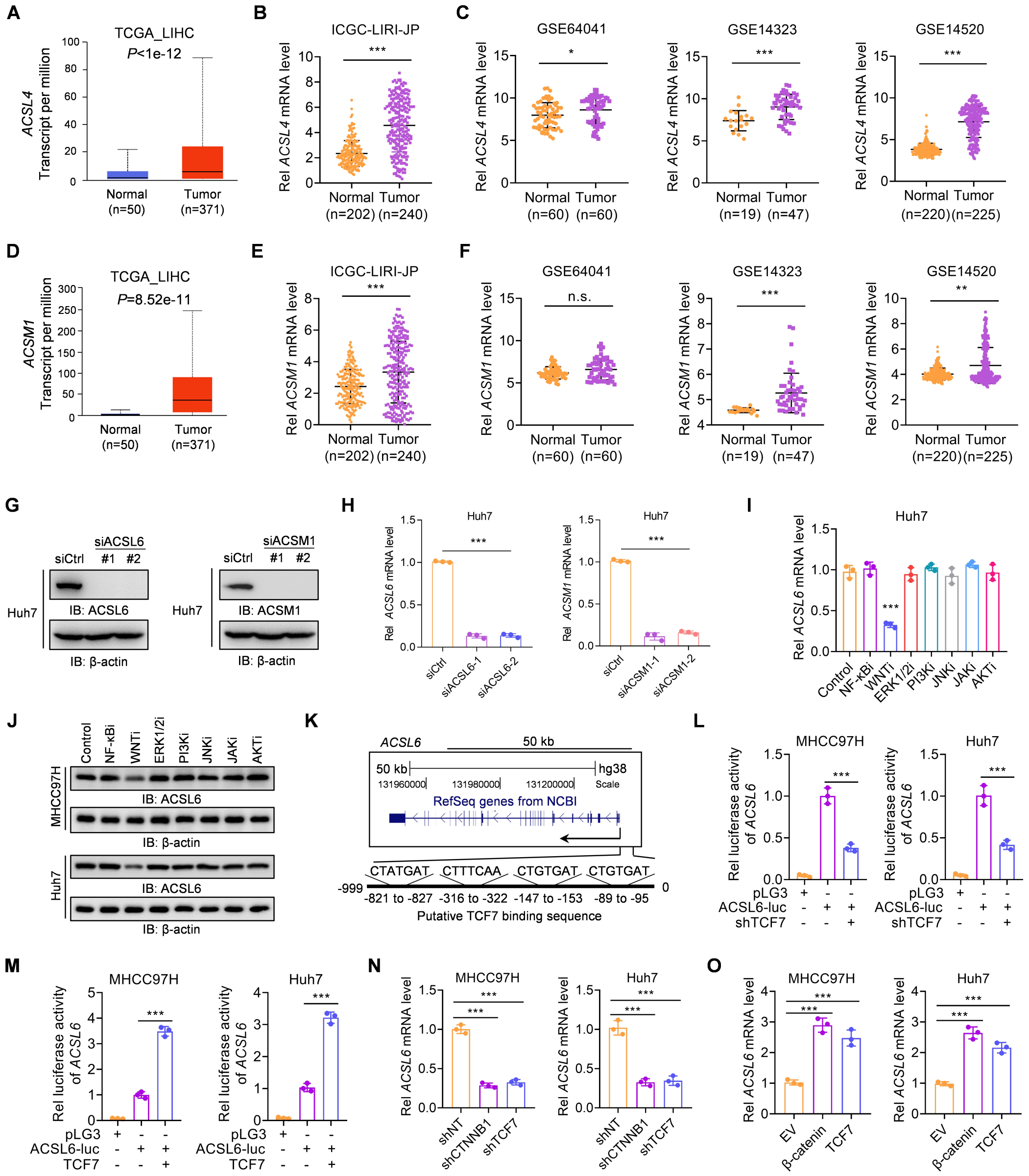

Fig. S1. ACSL6 is upregulated in liver cancer. (**A** to **C**) Analyses of *ACSL4* expression in liver tumor and adjacent nontumor tissues from TCGA (A), ICGC (B) and GEO (GSE64041, GSE14323 and GSE14520) (C) databases. (**D** to **F**) Analyses of *ACSM1* expression in liver tumor and adjacent nontumor tissues from TCGA (D), ICGC (E), and GEO (GSE64041, GSE14323 and GSE14520) (F) databases. (**G** and **H**) Protein (G) and mRNA expression (H) of the indicated genes in Huh7 cells transfected with the control siRNA (siCtrl) or siRNAs targeting ACSL6 or ACSM1. (**I** and **J**) QPCR (I) and immunoblotting (J) analyses of ACSL6 expression in MHCC97H or Huh7 cells stimulated with inhibitors targeting NF-κB, WNT, ERK1/2, PI3K, JNK, JAK, and AKT. (**K**) The TCF7 DNA-binding sites in the *ACSL6* promoter were identified. (**L**) Luciferase assay of *ACSL6* promoter-driven reporters in shNT and shTCF7 MHCC97H or Huh7 cells. (**M**) Luciferase analyses of *ACSL6* promoter-driven reporters in control or TCF7-overpressing MHCC97H and Huh7 cells. (**N**) QPCR analyses of the *ACSL6* expression in shNT, shCTNNB1 and shTCF7 MHCC97H or Huh7 cells. (**O**) QPCR analyses of the *ACSL6* expression in EV, β-catenin and TCF7 overexpressing MHCC97H or Huh7 cells. *P<0.05, **P < 0.01, ***P < 0.001, n.s. = non-significance. Student's t-test (A-F, L, M), one-way ANOVA (H, I, N, O).

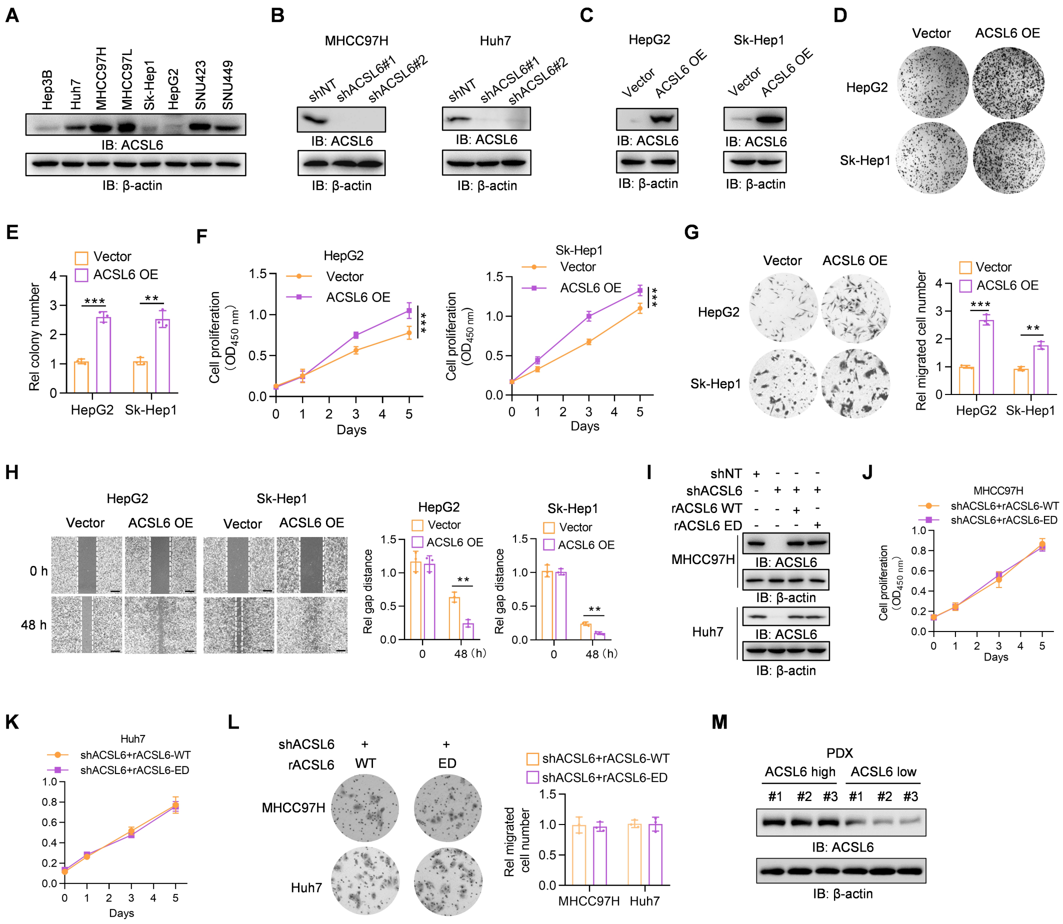

Fig. S2. ACSL6 promotes cell proliferation and migration *in vitro* and facilitates liver cancer growth and metastasis *in vivo*. (**A**) Immunoblotting analyses of ACSL6 expression in various liver cancer cell lines. (**B**) Immunoblotting analyses of ACSL6 expression in shNT or shACSL6 MHCC97H and Huh7 cells. (**C**) Immunoblotting analyses of ACSL6 expression in control (vector) and ACSL6-overexpressing HepG2 and Sk-Hep1 cells. (**D** to **F**) Colony formation (D, E) and CCK-8 analyses (F) were performed to evaluate the growth of vector and ACSL6-overexpressing HepG2 and Sk-Hep1 cells. (**G** and **H**) Transwell (G) and wound healing (H) assays were used to evaluate the migration ability of vector and ACSL6 overexpressed HepG2 and Sk-Hep1 cells. (**I**) Immunoblotting analyses of ACSL6 expression in shNT, shACSL6, and shACSL6 reconstituted with rACSL6 WT or ED MHCC97H and Huh7 cells. (**J** to **L**) CCK-8 (J, K) and transwell (L) assays of shACSL6 reconstituted with rACSL6 WT or ED in MHCC97H and Huh7 cells. (**M**) ACSL6 protein expression in PDX model mice. $^{**}P<0.01$ and $^{***}P<0.001$. Student's t-test (E, G, H, L), or two-way

ANOVA (F, J, K).

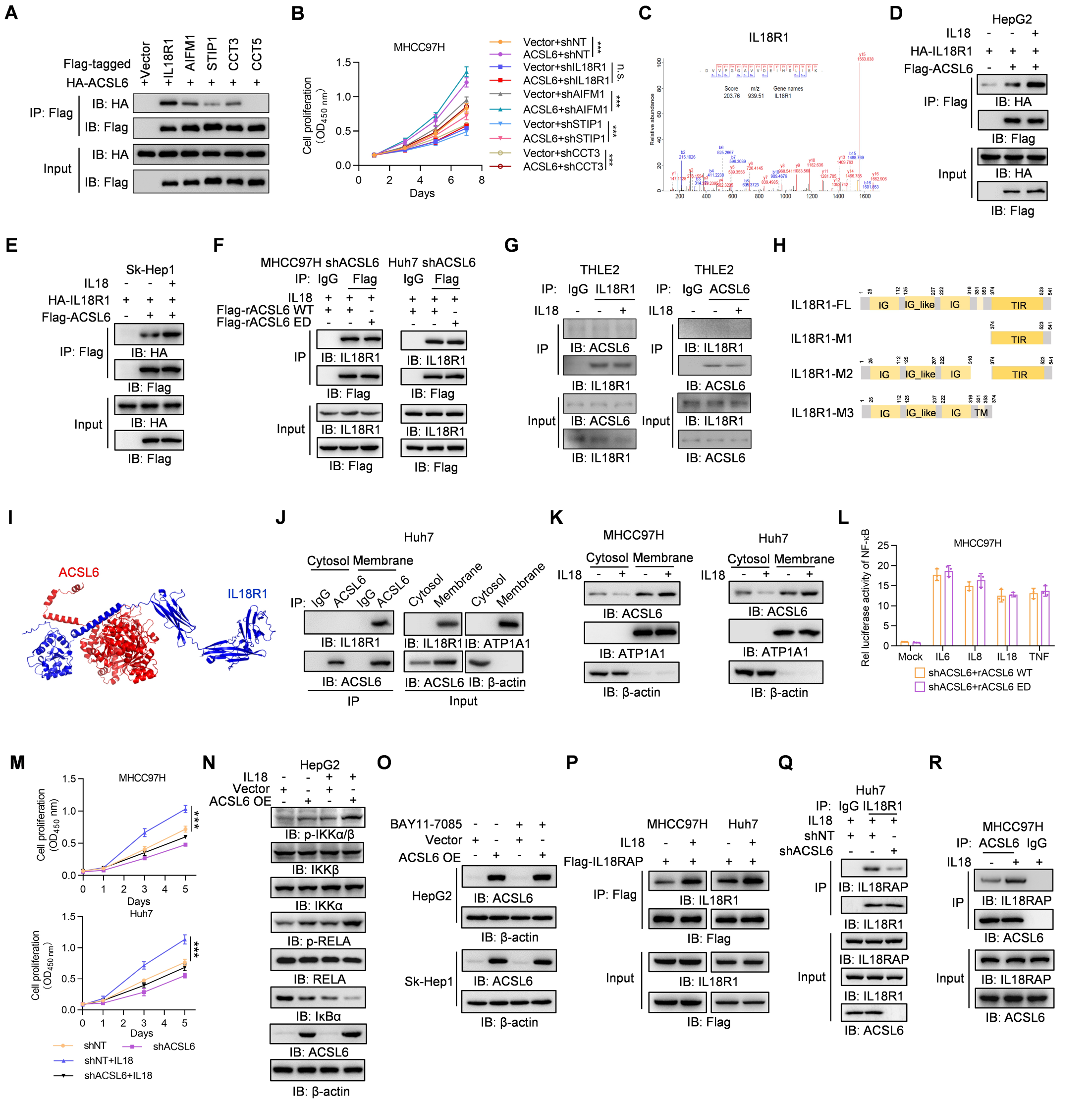

Fig. S3. ACSL6 interacts with IL18R1 to activate the IL18-IL18R1-NF-κB signaling in liver cancer cells. (**A**) HA-ACSL6-expressing MHCC97H cells were transfected with Flag-tagged expression plasmids, and coIP was performed. (**B**) Vector and ACSL6-overexpressing MHCC97H cells were infected with lentiviruses expressing shNT, shIL18R1, shAIFM1, shSTIP1 and shCCT3. CCK-8 assays were performed to evaluate the growth. (**C**) Mass spectrometry analyses revealed that the protein bound to Flag-ACSL6 was IL18R1. (**D** and **E**) HepG2 and Sk-Hep1 cells overexpressing HA-IL18R1 were infected with a lentivirus expressing Flag-ACSL6 and treated with or without 20 ng·ml^{-1} IL18 for 1 h. CoIP was performed. (**F**) ACSL6-depleted MHCC97H and Huh7 cells reconstituted with Flag-rACSL6 WT or ED were treated with 20 ng·ml^{-1} IL18 for 1 h. CoIP was performed. (**G**) IL18R1 or ACSL6 was immunoprecipitated from nontumorigenic THLE2 liver cells treated with or without 20 ng·ml^{-1} IL18 for 1 h. CoIP was performed. (**H**) Structural diagrams of full-length IL18R1 and IL18R1 mutants. (**I**) Computational model of the ACSL6 and IL18R1 interaction structure predicted using ZDOCK and PyMol software. (**J**) The membrane and cytosolic fractions were separated from Huh7 cells, and coIP was performed. (**K**) Immunoblotting analyses of the indicated proteins in the membrane and cytosolic fractions of MHCC97H and Huh7 cells treated with or without 20 ng·ml^{-1} IL18 for 1 h. (**L**) Luciferase analyses of NF-κB-luc from shACSL6 MHCC97H cells reconstituted with rACSL6 WT or ED. The cells were treated with 20 ng·ml^{-1} IL6, IL8, IL18, or TNF for 12 h. (**M**) CCK-8 assay of the growth of shNT and shACSL6 MHCC97H and Huh7 cells treated with or without 20 ng·ml^{-1} IL18. (**N**) Immunoblotting analyses of the levels of the indicated proteins in vector and ACSL6-overexpressing HepG2 cells treated with 20 ng·ml^{-1} IL18 for 1 h. (**O**) Immunoblotting analyses of the levels of indicated proteins in vector and ACSL6-overexpressing HepG2 and Sk-Hep1 cells treated with or without 10 μM BAY 11-7085 for 24 h. (**P**) MHCC97H and Huh7 cells expressing Flag-IL18RAP were treated with or without 20 ng·ml^{-1} IL18 for 1 h, and coIP was performed. (**Q**) Huh7 cells expressing shNT or shACSL6 were treated with 20 ng·ml^{-1} IL18 for 1 h, and coIP was performed. (**R**) MHCC97H cells were treated with or without 20 ng·ml^{-1} IL18 for 1 h, and coIP was performed. **P <0.01 and ***P <0.001. two-way ANOVA (B, M), or Student's t-test (L).

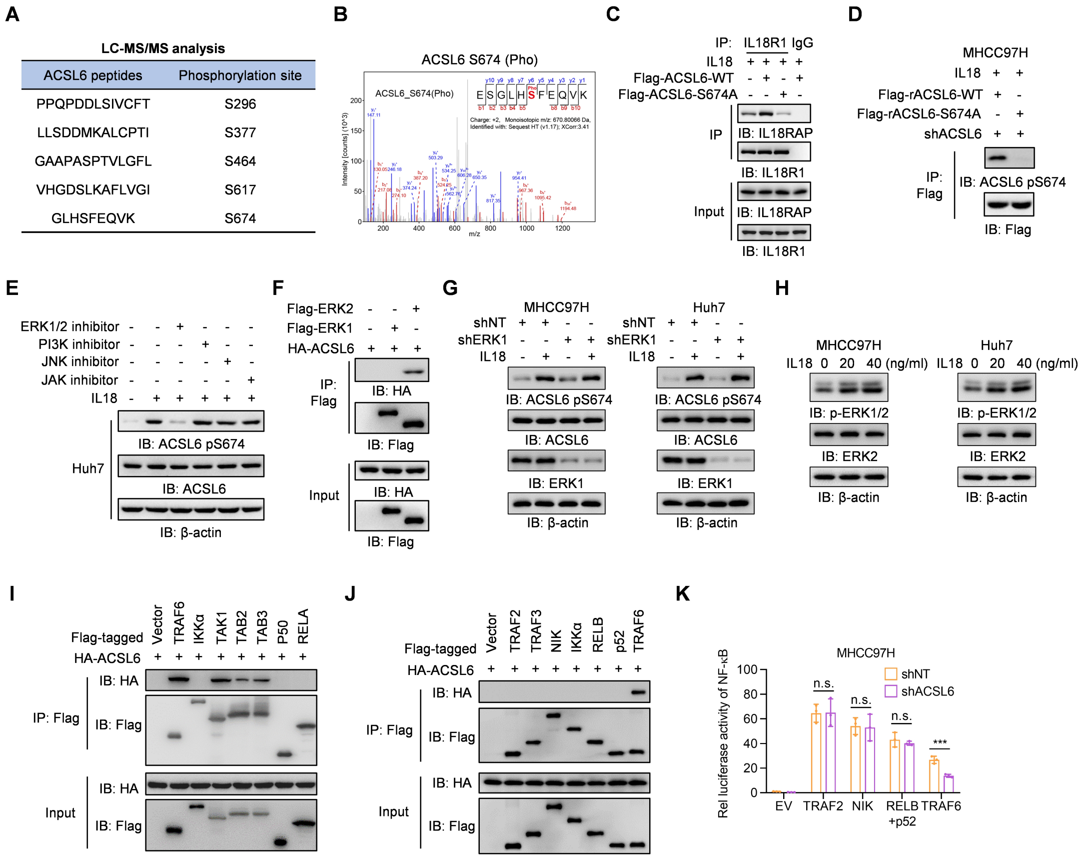

Fig. S4. IL18 induces ACSL6 pS674 to activate NF-κB signaling. (**A**) Flag-ACSL6 was immunoprecipitated from MHCC97H cells treated with or without 20 ng·ml^{-1} IL18 for 1 h. The phosphorylated residues after IL18 stimulation were identified by mass spectrometry, and the S296, S377, S464, S617 and S674 phosphorylation sites in ACSL6 were determined. (**B**) LC-MS/MS spectrum of modified ACSL6 pS674. (**C**) MHCC97H cells overexpressing Flag-ACSL6-WT or S674A were treated with 20 ng·ml^{-1} IL18 for 1 h, and coIP was performed. (**D**) ACSL6-depleted MHCC97H cells were infected with Flag-rACSL6 WT or S674A and treated with 20 ng·ml^{-1} IL18 for 1 h. CoIP was performed. (**E**) MHCC97H cells were treated with or without the indicated inhibitors for 6 h and then treated with 20 ng·ml^{-1} IL18 for 1 h. CoIP was performed. (**F**) HA-ACSL6-expressing MHCC97H cells were transfected with Flag-tagged vector, ERK1 or ERK2 plasmid, and coIP was performed. (**G**) MHCC97H and Huh7 cells expressing shNT or shERK1 were treated with or without 20 ng·ml^{-1} IL18 for 1 h. Immunoblotting analyses were performed with indicated antibodies. (**H**) MHCC97H and Huh7 cells were treated with or without different concentrations of IL18 for 1 h. Immunoblotting analyses were performed with indicated antibodies. (**I**)

HA-ACSL6-expressing MHCC97H cells were transfected with Flag-tagged NF-κB expression plasmids, and coIP was performed. (**J**) HA-ACSL6-expressing MHCC97H cells were transfected with Flag-tagged non-canonical NF-κB expression plasmids, and coIP was performed. (**K**) Luciferase analyses of NF-κB-luc in shNT and shACSL6 MHCC97H cells transfected with Flag-tagged non-canonical NF-κB expression plasmids and canonical NF-κB expression plasmids TRAF6. ***P <0.001, and n.s.=non-significant. Student's t-test (K).

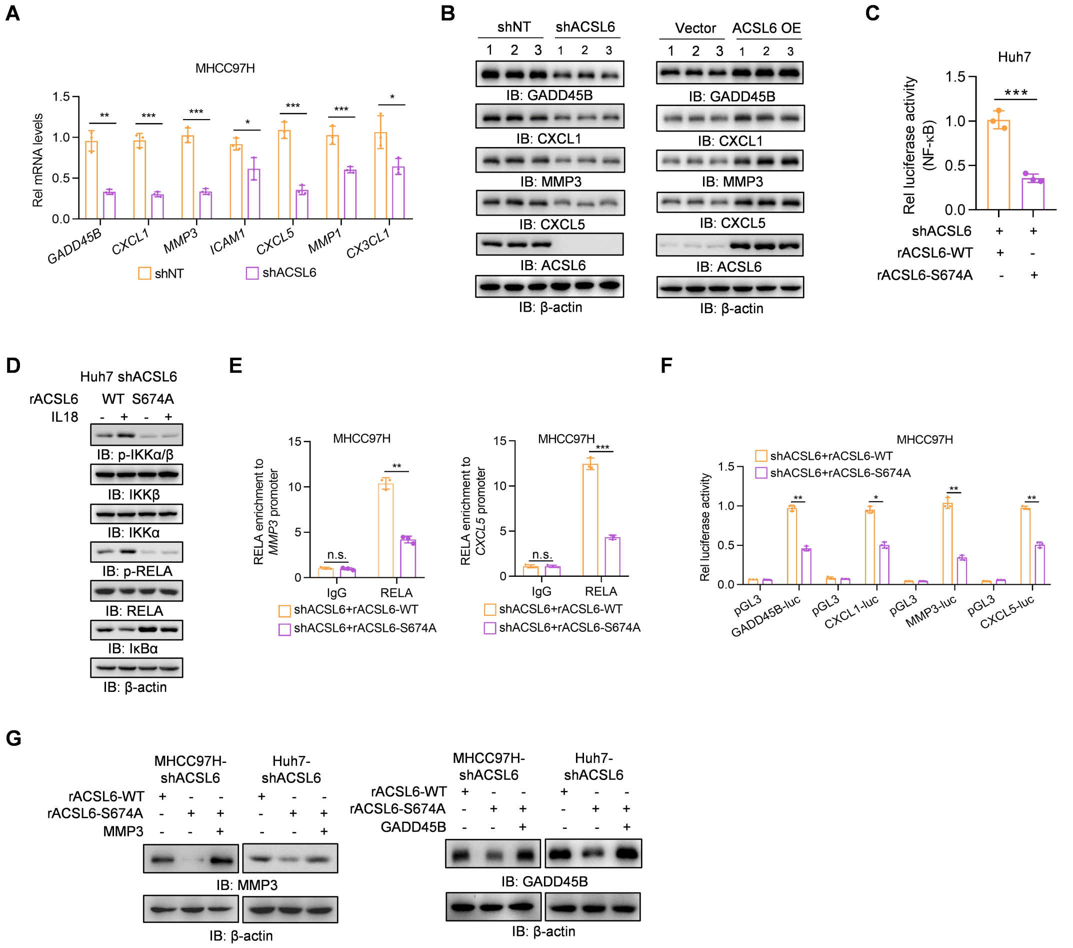

Fig. S5. ACSL6 promotes CXCL1/CXCL5 expression through the activation of NF-κB signaling. (**A**) QPCR analyses of the mRNA expression of indicated genes in shNT and shACSL6 MHCC97H cells. (**B**) Immunoblotting analyses of the levels of indicated proteins in subcutaneous xenografts tumors with ACSL6 knockdown or overexpression. (**C**) Luciferase analyses of NF-κB-luc activity in ACSL6-depleted Huh7 cells reconstituted with rACSL6 WT or S674A. (**D**) Immunoblotting analyses of the levels of indicated proteins in ACSL6-depleted Huh7 cells reconstituted with rACSL6 WT or S674A and treated with or without 20 ng·ml^{-1} IL18 for 1 h. (**E**) ChIP–qPCR analyses were performed with the indicated antibodies, and DNA was amplified with primers targeting the positive sites in the indicated genes in MHCC97H cells. (**F**) Luciferase analyses of GADD45B-luc, CXCL1-luc, MMP3-luc and CXCL5-luc activity in ACSL6-depleted MHCC97H cells reconstituted with rACSL6 WT or S674A. (**G**) Immunoblotting analyses of the levels of indicated proteins in ACSL6-depleted MHCC97H and Huh7 cells reconstituted with rACSL6

WT, S674A, S674A with MMP3 or S674A with GADD45B. **P* <0.05, ***P* <0.01, ****P* <0.001. Student's t-test (A, C, F), one-way ANOVA (E).

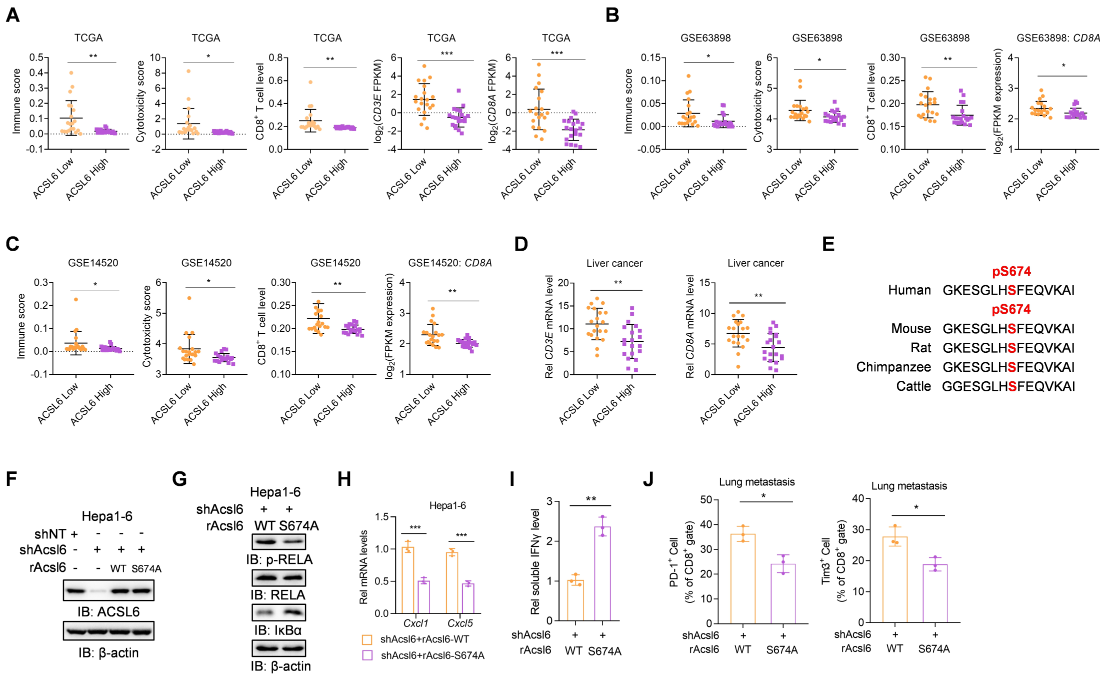

Fig. S6. ACSL6 expression inversely correlates with CD8^{+} T cell levels. (**A**) Associations of ACSL6 expression with the immune score, cytotoxicity score, CD8^{+} T-cell level, and the expression levels of *CD3E* and *CD8A* in TCGA-LIHC cohort. (**B** and **C**) Comparative analyses of the associations of ACSL6 expression with the immune score, cytotoxicity score, CD8^{+} T cells and *CD8A* expression in patients represented in the GSE63898 (B) and GSE14520 (C) datasets. (**D**) Analyses of *CD3E* and *CD8A* expression in liver cancer patients with high or low *ACSL6* expression. (**E**) Sequence alignment of the ACSL6 S674 peptides in the indicated species. (**F**) Immunoblotting analyses of ACSL6 expression in shNT, shAcsl6, and shAcsl6 reconstituted with rAcsl6 WT or S674A Hepa1-6 cells. (**G** and **H**) Immunoblotting analyses using indicated antibodies (G) and qPCR analyses of *Cxcl1* and *Cxcl5* expression (H) in Acsl6-depleted Hepa1-6 cells reconstituted with rAcsl6-WT or S674A. (**I**) Measurement of the concentration of IFNγ in the indicated tumors using ELISA. (**J**) Flow cytometry analyses of tumor-infiltrating PD-1^{+}CD8^{+} and Tim3^{+}CD8^{+} T cells in metastatic lung nodules from C57BL/6 mice. **P* <0.05, ***P* <0.01 and ****P* <0.001. Student's t-test (A-D, H-J).

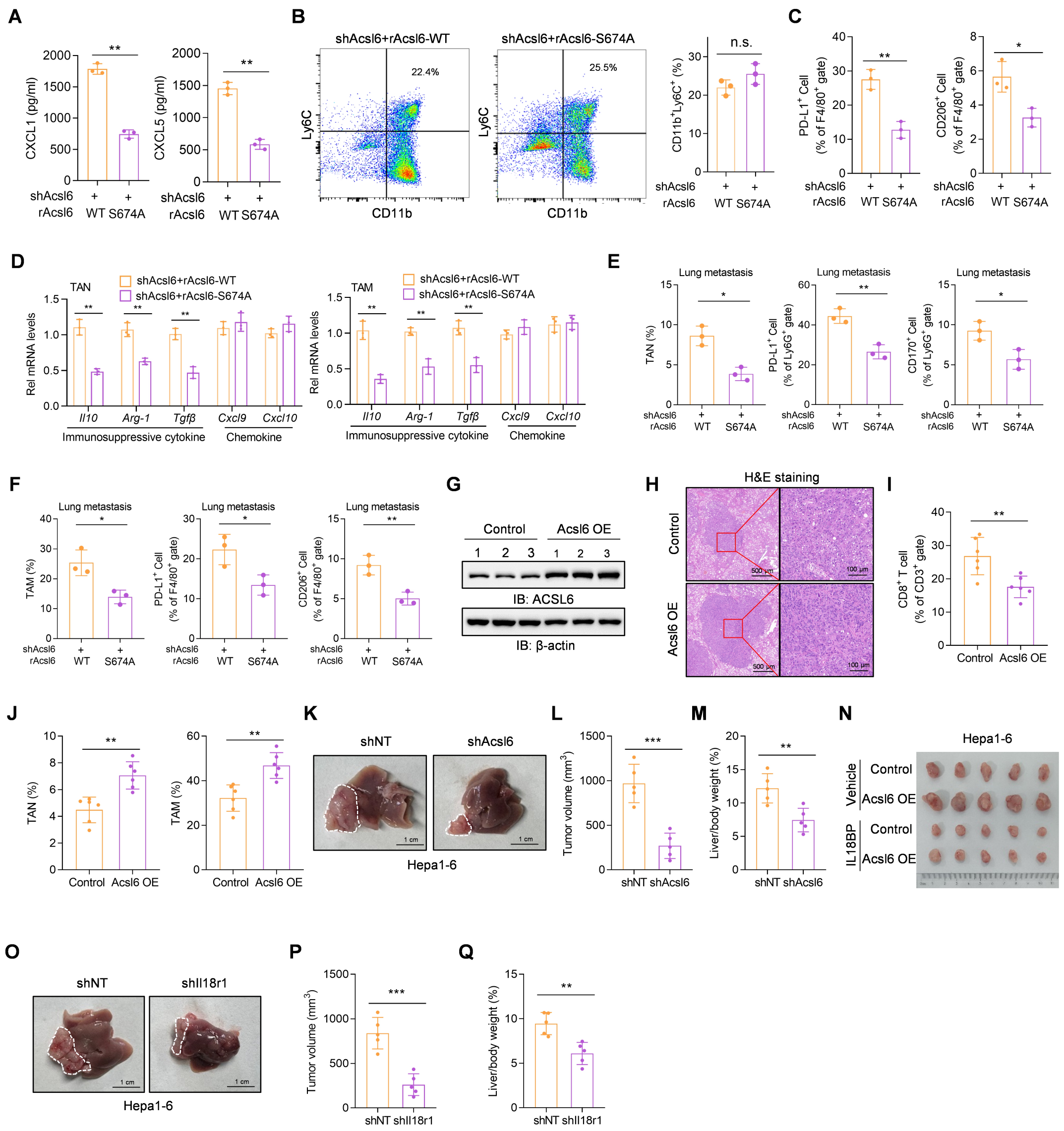

Fig. S7. ACSL6 pS674 promotes TANs and TAMs recruitment. (**A**) ELISAs of the concentrations of CXCL1 and CXCL5 in the indicated tumors. (**B** and **C**) Analysis of tumor-infiltrating CD11b^{+}Ly6C^{+} cells (B), PD-L1^{+}F4/80^{+} cells and CD206^{+}F4/80^{+} cells (C) in the indicated tumors. (**D**) The mRNA expression of indicated genes in TANs and TAMs from indicated tumors. (**E** and **F**) Flow cytometry analyses of tumor-infiltrating TANs, PD-L1^{+}Ly6G^{+} and CD170^{+}Ly6G $^{+}$ (E), and TAMs, PD-L1^{+}F4/80^{+} and CD206^{+}F4/80^{+} (F) in metastatic lung nodules from C57BL/6 mice. (**G** to **J**) Hydrodynamic transfection of AKT/NRAS/SB/Vector (control) or AKT/NRAS/SB/Acsl6 plasmids to establish liver cancer mouse model. Immunoblotting analyses of ACSL6 expression in indicated tumors (G). Representative images of H&E staining of mouse liver sections (H). Flow cytometry analyses of tumor- infiltrating $CD8^+$ T cells (I), TANs and TAMs (J). (**K** to **M**) Assessment of the impact of Acsl6 knockdown on liver cancer orthotopic xenografts using Hepa1-6 cells expressing either shNT or shAcsl6 in C57BL/6 mice. Representative images (K), tumor volumes (L), and liver weight/body weight ratios (M) in orthotopic models. (**N**) Subcutaneous injection of control or Acsl6-OE Hepa1-6 cells into C57BL/6 mice and then with or without IL18BP. Tumor images are shown. (**O** to **Q**) Assessment of the impact of Il18r1 knockdown in liver cancer orthotopic xenografts generated from Hepa1-6 cells expressing either shNT or shIl18r1 in C57BL/6 mice. Representative images (O), tumor volumes (P), and liver weight/body weight ratios (Q) in orthotopic models. G-J, n=6; K-Q, n=5. *P <0.05, **P <0.01, ***P <0.001. Student's t-test (A-F, I, J, L, M, P, Q).

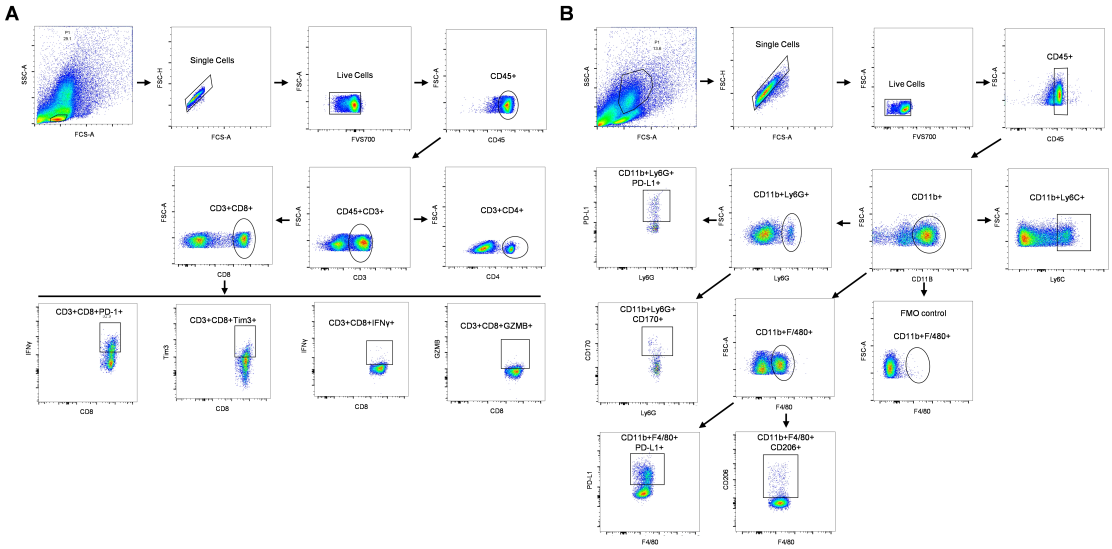

Fig. S8. Gating strategies used in FACS analyses. (**A**) Gating strategy for analyzing the populations of $CD4^+$ T cells, $CD8^+$ T cells, $IFN\gamma^+CD8^+$ T cells, $GZMB^+CD8^+$ T cells, $PD\text{-}1^+CD8^+$ T cells, and $Tim3^+CD8^+$ T cells in tumors. (**B**) Gating strategy for analyzing the populations of TANs ($CD11b^+Ly6G^+$), TAMs ($CD11b^+F4/80^+$), $CD11b^+Ly6C^+$ cells, $PD\text{-}L1^+$ TANs, $CD170^+$ TANs, $PD\text{-}L1^+$ TAMs, and $CD206^+$ TAMs in tumors.

Number	Gene	Entrze_ID
1	ACSBG1	23205
2	ACSBG2	81616
3	ACSF2	80221
4	ACSF3	197322
5	ACSL1	2180
6	ACSL3	2181
7	ACSL4	2182
8	ACSL5	51703
9	ACSL6	23305
10	ACSM1	116285
11	ACSM2A	123876
12	ACSM3	6296
13	ACSM4	341392
14	ACSM5	54988
15	ACSS1	84532
16	ACSS2	55902
17	ACSS3	79611

Table S1. The list of known 17 acyl-CoA synthetase

Identifier	Sequences (5'-3')
siACSL6#1	CCUCCUGAUGCAGUCAGAAGAAGUA
siACSL6#2	CGGACUUCUCCAGCACAAUUGUAAA
siACSM1#1	GGGACCUAGUUCAGCUACGUCCUAA
siACSM1#2	GGACCUAGUUCAGCUACGUCCUAAA
shACSL6#1	CCAGGCAAACACACCATTAAA
shACSL6#2	GCAGGTTAAAGCCATTCACAT
shCTNNB1	TTGTTATCAGAGGACTAAATA
shTCF7	TCCAGCACACTTGTCTAATAA
shIL18R1	GCTCACAATTTGAAGATGAAA
shERK2	GCTCACAATTTGAAGATGAAA
shERK1	GCAGCTGAGCAATGACCATAT
shAcsl6	GCCAGAGAAGATCGAGAACAT

Table S2. The sequences of shRNAs and siRNAs

Gene	Forward (5'-3')	Reverse (5'-3')
ACTB	GCGTGACATTAAGGAGAAG	GAAGGAAGGCTGGAAGAG
ACSL6	TCTTCCTCGTGTCGGG	CTCAGGCAGTCGCAGTA
ACSM1	TATGTACTGGACTACTGGGCTC	GGGTTAGGTCTCCCATCTCTCT
GADD45B	TACGAGTCGGCCAAGTTGATG	GGATGAGCGTGAAGTGGATTT
CXCL1	TGCTCCTGCTCCTGGTAG	TGGCTATGACTTCGGTTTGG
MMP3	GGAAAACCCACCTTACA	TCATACAGCCTGGAGAAT
CXCL5	AGCTGCGTTGCGTTTGTTTAC	TGGCGAACACTTGCAGATTAC
MMP1	CTGAAAGTGACTGGGAAAC	TGAGGACAAACTGAGCC
ICAM1	ATGCCCAGACATCTGTGTCC	GGGGTCTCTATGCCCAACAA
CX3CL1	CGCGCAATCATCTTGGAGAC	CATCGCGTCCTTGACCCAT
TNF	AGTGAAGTGCTGGCAACCAC	GAGGAAGGCCTAAGGTCCAC
CD3E	TGCTGCTGGTTTACTACTGGA	GGATGGGCTCATAGTCTGGG
CD8A	ATGGCCTTACCAGTGACCG	AGGTTCCAGGTCCGATCCAG
IL10	GCTCTTACTGACTGGCATGAG	CGCAGCTCTAGGAGCATGTG
Arg-1	CTCCAAGCCAAAGTCCTTAGAG	AGGAGCTGTCATTAGGGACATC

Tgfβ	CTCCCGTGGCTTCTAGTGC	GCCTTAGTTTGGACAGGATCTG
Cxcl9	TCCTTTTGGGCATCATCTTCC	TTTGTAGTGGATCGTGCCTCG
Cxcl10	CCAAGTGCTGCCGTCATTTTC	GGCTCGCAGGGATGATTTCAA

Table S3. Quantitative real-time qPCR primers

Antibody	Source	RRID	Company
ACSL6	Rabbit pAb (#NBP1-89269)	AB_11033373	Novus Biologicals, USA
ACSL6	Rabbit pAb (#PA5-101652)	AB_2851086	ThermoFisher Scientific, USA
ACSM1	Rabbit pAb (#NBP2-15254)	AB_3099547	Novus Biologicals, USA
β-actin	Mouse mAb (#A1978)	AB_476692	Sigma Aldrich, USA
β-catenin	Rabbit pAb (#A0316)	AB_2757122	Abclonal Technology, China
TCF7	Mouse mAb (#sc-271453)	AB_10649799	Santa Cruz Biotechnology, USA
p-ERK1/2	Rabbit mAb (#4370)	AB_2315112	Cell Signaling Technology, USA
ERK1	Rabbit mAb (#A19561)	AB_2862668	Abclonal Technology, China
ERK2	Rabbit pAb (#A0229)	AB_2757042	Abclonal Technology, China
IL18R1	Rabbit pAb (#DF4712)	AB_2837063	Affinity Biosciences, China
IL18R1	Rabbit pAb (#PA5-96194)	AB_2807996	ThermoFisher Scientific, USA
IL18RAP	Rabbit pAb (#PA5-72578)	AB_2718432	ThermoFisher Scientific, USA
Phospho-Ser	Rabbit mAb (#ICP9806)	AB_2801332	ImmuneChem, Canada
Phospho-Tyr	Mouse mAb (#sc-508)	AB_628122	Santa Cruz Biotechnology, USA
Phospho-Thr	Mouse mAb (#sc-5267)	AB_628121	Santa Cruz Biotechnology, USA
ACSL6	Rabbit pAb (N/A)	N/A	Abclonal Technology,

pS674			China
ATP1A1	Rabbit pAb (#14418-1-AP)	AB_2227873	Proteintech Group, USA
CXCL1	Rabbit pAb (#12335-1-AP)	AB_2087568	Proteintech Group, USA
GADD45B	Mouse mAb (#sc-377311)	AB_3099548	Santa Cruz Biotechnology, USA
CXCL5	Rabbit pAb (#DF9919)	AB_2843113	Affinity Biosciences, China
MMP3	Rabbit pAb (#A1202)	AB_2758931	Abclonal Technology, China
phospho-IKKα/β (Ser176/180)	Rabbit mAb (#2697)	AB_2079382	Cell Signaling Technology, USA
IKKβ	Rabbit mAb (#8943)	AB_11024092	Cell Signaling Technology, USA
IKKα	Rabbit mAb (#61294)	AB_2799606	Cell Signaling Technology, USA
Phospho-RELA (Ser536)	Rabbit mAb (#3033)	AB_331284	Cell Signaling Technology, USA
RELA	Rabbit mAb (#8242)	AB_10859369	Cell Signaling Technology, USA
Flag-Tag	Mouse mAb (#F1804)	AB_262044	Sigma Aldrich, USA
HA-Tag	Rabbit mAb (#3724)	AB_1549585	Cell Signaling Technology, USA

Table S4. Antibodies used for IP and IB analyses

Other Supplementary Materials for this manuscript includes the following:

Data S1. Numerical data for quantification